A mobile charge densities in harmonic oscillators (MCDHO) molecular model for numerical simulations

Saint-Martin, H.; Hernandez-Cobos, J.; Bernal-Uruchurtu, M. I.; Ortega-Blake, I.; Berendsen, H. J. C.

Published in:
Journal of Chemical Physics

DOI:
10.1063/1.1324711

A mobile charge densities in harmonic oscillators (MCDHO) molecular model for numerical simulations: The water–water interaction

Humberto Saint-Martin, Jorge Hernández-Cobos, Margarita I. Bernal-Uruchurtu, Iván Ortega-Blake, and Herman J. C. Berendsen

Citation: J. Chem. Phys. **113**, 10899 (2000); doi: 10.1063/1.1324711
View online: https://doi.org/10.1063/1.1324711
View Table of Contents: http://aip.scitation.org/toc/jcp/113/24
Published by the American Institute of Physics

A mobile charge densities in harmonic oscillators (MCDHO) molecular model for numerical simulations: The water–water interaction

Humberto Saint-Martin[a] and Jorge Hernández-Cobos
Centro de Ciencias Físicas, Universidad Nacional Autónoma de México, Apartado Postal 48-3, Cuernavaca, Morelos 62251, México

Margarita I. Bernal-Uruchurtu[b]
UMR CNRS-UHP No. 7565 Intitut Nancéien de Chimie Moléculaire, Université Henri Poincaré-Nancy 1, BP 239, 54506 Vandoeuvre-lès-Nancy Cedex, France

Iván Ortega-Blake
Centro de Ciencias Físicas, Universidad Nacional Autónoma de México, Apartado Postal 48-3, Cuernavaca, Morelos 62251, México

Herman J. C. Berendsen
Department of Biophysical Chemistry, Rijksuniversiteit Groningen and BIOSON Research Institute, Nijenborgh 4, 9747 AG Groningen, The Netherlands

(Received 20 October 1999; accepted 20 September 2000)

In this work we present a new proposal to model intermolecular interactions and use it for water molecules. The parameters of the model were fitted to reproduce the single molecule's electrostatic properties, a sample of 352 points in a refined *ab initio* single molecule deformation potential energy surface (PES), and the theoretical limit of the dimerization energy, −20.8 kJ/mol. The model was able to reproduce a sample of 180 additional points in the single molecule deformation PES, and 736 points in a pair-interaction surface computed at the MP2/aug-cc-pVQZ′ level with the counterpoise correction. Though the model reproduced the diagonal of the polarizability tensor, it could account for only 60% of the three-body nonadditive contributions to the interaction energies in 174 trimers computed at the MP2/6-311++$(2d,2p)$ level with full counterpoise correction, but reproduced the four-body nonadditivities in 34 tetramers computed at the same level as the trimers. The model's predictions of the structures, energies, and dipoles of small clusters resulted in good agreement with experimental data and high quality *ab initio* calculations. The model also reproduced the second virial coefficient of steam at various temperatures, and the structure and thermodynamical properties of liquid water. We found that the short-range water–water interactions had a critical influence on the proper performance of the model. We also found that a model based on the proper intermolecular interactions requires the inclusion of intramolecular flexibility to be adequate. [S0021-9606(00)50847-2]

I. INTRODUCTION

Due to its relevance as an important constituent of living organisms, of earth, and even of interstellar space, as well as to its unique macroscopic and microscopic properties, water is probably the most studied substance of all.[1] In spite of vast literature about the subject,[2] the description of its behavior in various phases still poses unresolved questions. The development of more refined techniques has allowed the experimental study of the single molecule properties,[3–7] of the water dimer,[8,9] and more recently of other water clusters, from the trimer to the decamer.[10–18] It has also been possible to make more accurate measurements of the structure of liquid water under ambient and supercritical conditions.[19] These combinations of new experimental data and more precise quantum calculations[20–32] calls for more refined models for the intermolecular interaction.[33–35]

The water models fitted to reproduce experimental data of condensed phases (of which a few examples are ST2,[36] SPC,[37] and TIP3P;[38] for a review see Refs. 39 and 40) usually produce single molecule properties that correspond to the averages of the molecules in the condensed phases; for instance, the dipole moment is between 2.2 and 2.6 D, instead of 1.85 D. Moreover, because they are pair-effective potentials, they also average the many-body nonadditive contributions to the energy, producing an overestimate of the pure pair interaction[41] that yields a poor comparison to *ab initio* surfaces and to the second virial coefficient, for instance. The inclusion of more complex effects in these potentials, such as the energetic cost of polarization, the polarizability or the flexibility of the molecule, requires a modification of the parameters and of the analytical formulas (e.g., PE,[42] SPC/E,[43] TIP4Pfq).[44]

On the other hand, the *ab initio* models in principle allow a stepwise approach that successively includes increasingly complex effects, from pure pair interactions to polarizability, many-body nonadditive contributions, and flexibility.

[a]Electronic mail: humberto@fis.unam.mx
[b]On leave from Centro de Investigaciones Químicas, Universidad Autónoma del Estado de Morelos, Cuernavaca, Morelos México.

Such is the case of the MCY[45] potential that was fitted to an *ab initio* pair-interaction surface, and the following refinements NCC,[46] including many-body nonadditivity, and NCC_{vib},[46] that includes also flexibility. Other examples of *ab initio* derived models are the MCHO[47] and the NEMO[48] potentials. The *ab initio* models generally produce a much more structured liquid water and a higher pressure than the empirical models, and the main criticism against them is an insufficient sampling of the interaction surfaces; for instance, the original MCY was fitted to only 66 points in the pair-interaction surface. Of course, the more recent *ab initio* models make use of several hundred points; but a sampling of several thousands is needed for the numerical integration of the second virial coefficient. Moreover, though fitted to the pair interactions, the MCY model overestimates the second virial coefficient.[41] This is due to the fact that the *ab initio* calculation then used produced a water dimerization energy of -23.5 kJ/mol, in agreement with the experimental value available at that time;[9] but this data was obtained from an analysis of vibrational modes that required the subtraction of theoretically computed intramolecular frequencies. That is one of the reasons why in the past decade there has been a very intense effort to find the most accurate description of the dimerization energy, by means of *ab initio* calculations with increasingly larger basis sets,[20–26] and taking care of the basis set superposition error (BSSE),[26–28,49] that converge up to now to a value of -20.8 kJ/mol.

The alternative approach to perform classical numerical simulations with a quantum potential requires some approximate method and is thus equally affected by the same problem of accuracy. The first attempt was the Car–Parrinello[50] method that employs Kohn's density functional theory[51] for the quantum calculations; depending on the approximate functional form employed, the dimerization energy varies from -12 to -20 kJ/mol,[52] that would obviously lead to different structural and energetic predictions. Another problem is the reduced number of molecules that can be used in the simulation cell with this methodology, ranging from 32 to 125.[52–54]

Another different attempt to use a quantum potential is the truncated adiabatic basis set (TAB) scheme[55] that uses a cc-pVDZ basis set. It was applied to 128 rigid water molecules at various temperatures and produced generally good results, but flat rdf's. Though this approach might be promising, it is currently quite limited in the number of water molecules that can be included in the simulation. Hence, there are still efforts to design models that are fitted to *ab initio* surfaces.[56–59]

This last respect is the topic of the present work: here we address the problem of describing the collective behavior of water molecules under various conditions, with models that adjust the properties of the single molecule, the intramolecular relaxation predicted by the calculations, and the current theoretical limit on the structural and energetic predictions of the water dimer. In the next section we present the model we designed and discuss the fitting of its parameters. Then the model is tested in its ability to reproduce *ab initio* surfaces of pair interactions and three- and four-body nonadditive effects; the optimal structures and energies of some water clusters $(H_2O)_n$ (with $n \leqslant 6$), the second virial coefficient, and the structure and thermodynamic properties of liquid water under ambient conditions.

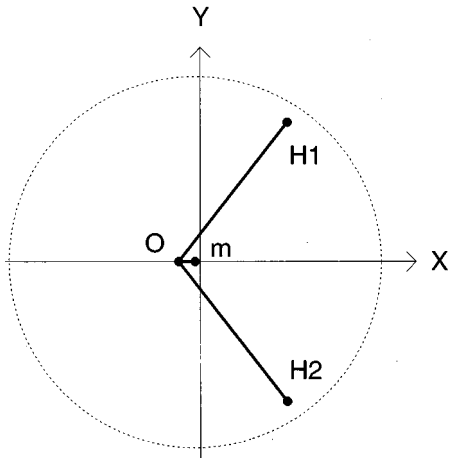

FIG. 1. Schematic representation of the MCDHO model. Positive charges Z are placed at the O, H1, and H2 nuclei, and a negative mobile charge q at the center m. The dashed line represents the spherical, exponentially decaying charge density centered on m. The electric dipole, quadrupole, and polarizability components in Table II are referred to this figure.

II. THE MCDHO MODEL

Because we wanted to explore the effects of successive refinements to the model, we started by reproducing the experimental single molecule dipole,[5] quadrupole,[4] and polarizability,[6] by considering three positively charged cores in the experimental geometry of the molecule,[3] and a negative mobile charge located close to the oxygen (Fig. 1). The representation of the water molecules with four sites is quite old,[60] and has been used in the MCY and TIP4P models, whereas the idea of mobile charges in harmonic oscillators is the main feature of the MCHO potential. Nevertheless, this latter considers both positive and negative mobile charges and is effectively a six-site model, which gives it enough flexibility to make it applicable to molecules different from water,[61] but it is rather costly.

A. The single molecule

The values of the two positive charges Z_O and Z_H on the nuclei, and the mobile negative charge q, as well as its position in the molecule, are completely determined by the single molecule's net charge, dipole, and quadrupole. The resulting value for q is somewhat large, $-3.90\ e$, but the difference $q - Z_O = -1.24\ e$ is similar to the net charge of the oxygen atom used in several models.

The next step was to include the polarizability; this was done by means of a harmonic oscillator potential that binds the mobile charge to the oxygen core. The anisotropy was taken into account by the interactions of the mobile charge with the hydrogen cores. This latter requires the screening of the coulombic interaction, or else the so-called *polarization catastrophe*[35] will occur: i.e., in response to a small perturbation the negative charge will collapse with one of the cores. In the present work we chose to model the screening

by considering the mobile charge q as a charge density ρ with spherical symmetry and an exponential, Slater-type radial decay of length λ:

$$\rho(r)=\frac{q}{\pi\lambda^3}\exp\left(-2\frac{r}{\lambda}\right), \quad \text{with} \quad q=4\pi\int_0^\infty \rho(r)r^2\,dr, \tag{1}$$

so there are two more parameters—the harmonic force constant k and the decay length λ—to fit the single molecule polarizability. The position of the mobile charge, corresponding to the zero of the force equation, is found by means of an iterative, self-consistent procedure, that requires the electrostatic field $\mathbf{E}$ and potential ϕ:

$$\mathbf{E}(r)=\frac{q}{r^2}\left\{1-\left[2\frac{r}{\lambda}\left(\frac{r}{\lambda}+1\right)+1\right]\exp\left(-2\frac{r}{\lambda}\right)\right\}\hat{\mathbf{r}}, \tag{2}$$

$$\phi(r)=\frac{q}{r}\left\{1-\left(\frac{r}{\lambda}+1\right)\exp\left(-2\frac{r}{\lambda}\right)\right\}. \tag{3}$$

The assumption of a rigid water molecule has been used extensively with good results, in spite of experimental data showing a significant deformation in the condensed phases.[62] Here we study this effect by including intramolecular flexibility in the model. This is done by allowing the electrostatic interaction between the charges on the nuclei, in addition to a Morse potential for the O–H bonds, and a fourth degree polynomial for the HOH angle. Thus, the model contains a nonzero energy for the isolated molecule, given by

$$\begin{aligned}U_m=&\frac{1}{2}kr_{\mathrm{O}}^2+\frac{Z_{\mathrm{H}}^2}{R_{1,2}}+\sum_{\beta=1}^{2}\left\{\frac{qZ_{\mathrm{H}}}{r_\beta}\left[1-\left(\frac{r_\beta}{\lambda}+1\right)\right.\right.\\&\left.\times\exp\left(-2\frac{r_\beta}{\lambda}\right)\right]+\frac{Z_{\mathrm{O}}Z_{\mathrm{H}}}{R_\beta}+D\{\exp[-2\gamma(R_\beta-r_e)]\\&\left.-2\exp[-\gamma(R_\beta-r_e)]\}\right\}+a_1(\theta-\theta_e)\\&+a_2(\theta-\theta_e)^2+a_3(\theta-\theta_e)^3+a_4(\theta-\theta_e)^4,\end{aligned} \tag{4}$$

that depends on r_{O}, the distance from q to the oxygen core, on $R_{1,2}$, the distance between hydrogen cores, on r_β, the distance from q to hydrogen core β, on R_β, the distance from the oxygen core to hydrogen core β, and on θ, the HOH angle. Using the intramolecular energy of the equilibrium monomer as a reference, the eight additional parameters, D, γ, r_e, θ_e, a_1, a_2, a_3, a_4, were fitted to 352 points generated by an analytical expression of a highly refined *ab initio* PES for the water molecule.[63] This sample includes deformations of $\pm10°$ of the HOH angle, and ±0.1 Å of the O–H bonds. These values are above the deformations in the condensed phases, and produce energies up to 42 kJ/mol above the equilibrium geometry. The values of these parameters are presented in Table I. The quality of the fit yields a root-mean-square error of $e_{\mathrm{rms}}=0.8$ kJ/mol. The comparison of the model to the equilibrium monomer is presented in Table II. It is worth noticing that the equilibrium monomer geometry found with a very large basis set[26] has shorter O–H bonds and a more open HOH angle than the experimental data, this latter corresponding to the analytical PES.[63]

TABLE I. Parameters of the MCDHO model to reproduce the single molecule.[a]

Z_{O}	2.660 000 00
Z_{H}	0.620 000 00
q	−3.900 000 00
k	1.480 000 00
λ	1.900 000 00
D	0.544 688 00
r_e	1.204 464 40
γ	1.167 763 60
θ_e	1.875 000 00
a_1	0.027 018 00
a_2	0.045 926 00
a_3	−0.018 199 00
a_4	−0.009 420 00

[a]Values are in a.u., the angle θ_e in radians ($\theta_e=107.43°$).

Though the model matches well the dipole and the quadrupole, its polarizability is slightly lower than the experimental data and closer to the *ab initio* values. However the experimental values are subject to significant uncertainties, as can be seen in Table II. These arise because the values are not measured directly, but interpreted from refraction or dielectric measurements, and averaged over the molecules in the sample.

B. The interaction energy of a cluster

The next step is to reproduce the pair interaction. At long distance ($r\geqslant5.5$ Å) this should be accomplished by the electrostatic properties of the single molecule; at medium distances ($2.7\text{ Å}\leqslant r\leqslant5.5$ Å), it can be obtained accurately from *ab initio* calculations with large basis sets at the MP2

TABLE II. Reproduction of the geometric and electrostatic features of the water monomer.[a]

Geometry	Ref. 26[b]	Ref. 31[c]	Experimental[d]	MCDHO
r(O–H)	0.9514	0.9589	0.9572±0.0003	0.9590
θ(H–O–H)	105.44	104.27	104.52±0.05	104.83
Multipoles[e]	**Ref. 24[f]**		**Experimental[g]**	**MCDHO**
μ_x	1.870		1.8546±0.0006	1.8494
Q_{xx}			−0.13±0.03	−0.24
Q_{yy}			2.63±0.02	2.67
Q_{zz}			−2.50±0.02	−2.44
Polarizability[e]	**Ref. 24[f]**	**Experimental[h]**	**Experimental[i]**	**MCDHO**
α_{xx}	1.384	1.468±0.003	1.426±0.135	1.357
α_{yy}	1.329	1.415±0.013	1.372±0.607	1.217
α_{zz}	1.450	1.528±0.013	1.483±0.607	1.482

[a]Distance in Å, angle in degrees, dipole in Debye, quadrupole in 10^{-26} esu cm^2, and polarizability in cm^3.
[b]Optimized with a very large UCV basis set (1046 functions); it does not correspond to the PES of Ref. 63.
[c]Optimized with an aug-cc-pVQZ basis set.
[d]Reference 3.
[e]The orientation corresponds to Fig. 1.
[f]Computed at the MP4/aug-cc-pVQZ level.
[g]Reference 5 for the dipole, and Ref. 4 for the quadrupole.
[h]Reference 6.
[i]Reference 7; see text for a discussion of the different experimental values of polarizabilities.

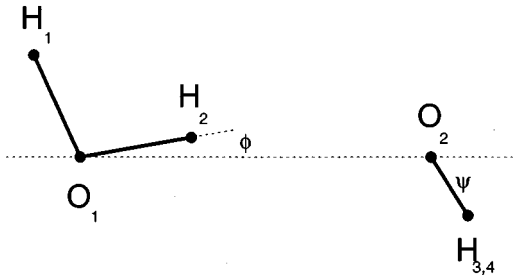

FIG. 2. Water dimer. The geometric parameters of Table III are referred to this figure.

level; however, the short-range interactions that are relevant in the liquid state are not so easy to reproduce accurately and there is a need for highly refined calculations.

As mentioned in the introduction, the theoretical limit for the dimerization energy of water is -20.8 kJ/mol, and it was obtained from high quality *ab initio* calculations,[26] as well as the corresponding equilibrium geometry (Fig. 2). To be able to reproduce the dimerization energy and the distance between oxygens, $r(O_1-O_2)$, some new terms had to be added to the model; after several attempts, we found that the interaction of the mobile charge density of one molecule with the three cores of another, required a decay length λ' different from that used for the intramolecular interaction. With respect to the intermolecular interaction between mobile charges in different molecules, instead of using the expression for the charge densities, that cannot be integrated analytically, we found it more convenient to consider them as closed shells, as in the shell model used in solid state physics,[64] so they behave as points with a 12–6–1 Lennard-Jones plus electrostatic potential. This can be done because the negative charges do not approach closely, and the effect of the screening is compensated by the Lennard-Jones terms. Nevertheless, this effect will have to be taken into account to be able to use the same type of model for other molecules, for which more than one mobile charge density per molecule might be required. In fact, this type of model has been successfully applied to diatomic molecules.[65,66]

Finally, the fine tuning of the angles ϕ and ψ in Fig. 2, required generic 12–6 terms in the O–H and H–H intermolecular interactions, so the analytical potential to compute the total energy of N molecules is

$$U_{\text{total}}=\sum_{n=1}^{N}\sum_{m=1}^{n-1}\left\{\left(\frac{A}{r_{nm}}\right)^{12}-\left(\frac{B}{r_{nm}}\right)^{6}+\frac{q^2}{r_{nm}}+\sum_{\beta\in m}\frac{qZ_\beta}{r_{n\beta}}\left[1-\left(\frac{r_{n\beta}}{\lambda'}+1\right)\exp\left(-2\frac{r_{n\beta}}{\lambda'}\right)\right]+\sum_{\alpha\in n}\sum_{\beta\in m}+\left[\left(\frac{A_{\alpha\beta}}{R_{\alpha\beta}}\right)^{12}-\left(\frac{B_{\alpha\beta}}{R_{\alpha\beta}}\right)^{6}+\frac{Z_\alpha Z_\beta}{R_{\alpha\beta}}\right]\right\}+\sum_{n=1}^{N}U_n, \tag{5}$$

where r_{nm} is the distance between the mobile charges in molecules n and m, $r_{n\beta}$, between the mobile charge in molecule n and the nucleus β in molecule m, $R_{\alpha\beta}$, between the nucleus α in molecule n and the nucleus β in molecule m. The first three rows in Eq. (5) correspond to the intermolecular interaction, and the last one to the intramolecular energy computed with Eq. (4) for each of the N molecules in the configuration determined by the positions of the nuclei, where the mobile charges have been taken to the equilibrium positions in the field of that configuration. The corresponding *interaction* energy is thus obtained from subtracting N times the reference energy of the equilibrium water monomer, U_e:

$$\Delta U=U_{\text{total}}-NU_e. \tag{6}$$

This expression allows to account for the energetic cost of both deformations and polarization.[43] The values of the parameters are presented in Table III.

TABLE III. Parameters of the MCDHO model to reproduce the pair interaction.[a]

λ'	1.110 100 00
A	3.204 242 95
B	2.027 670 94
A_{OH}	0
B_{OH}	1.194 170 49
A_{HH}	2.442 124 05
B_{HH}	0

[a]Values in a.u.

The reproduction of the dimer's energy, geometry, and total dipole, is shown in Table IV. There is a good general agreement, with an intermolecular O–O separation 0.009 Å shorter than the *ab initio* value, that is already shorter than the recommended value from experimental data. The angles ϕ and ψ are also well-reproduced, with differences relative to the *ab initio* values of $\Delta\phi=-0.5°$ and $\Delta\psi=4.3°$. The total dipole moment of the dimer is predicted as $\mu=2.681$ D, compared to the experimental value,[8] $\mu=2.643$ D, and an *ab initio* calculation[67] of $\mu=2.683$ D. The geometries of the two monomers are different from the *ab initio* results, which is not surprising because the single molecule reproduced by the model has a similar discrepancy with respect to the *ab initio* prediction with the same basis set used for the dimer.

TABLE IV. Reproduction of the water dimer.[a]

	Ref. 26[b]	Experimental[c]	MCDHO
$r(O_1-H_1)$	0.9506		0.9557
$r(O_1-H_2)$	0.9588		0.9704
$r(O_2-H_3)$	0.9529		0.9640
$\theta(H_1-O_1-H_2)$	105.51		103.95
$\theta(H_3-O_2-H_4)$	105.25		104.19
$r(O_1-O_2)$	2.925	2.952[d]	2.916
ϕ	4.3	0.0 ± 6.0	3.8
ψ	51.8	58.0 ± 6.0	56.1
Dimerization energy	-20.8	-22.6 ± 2.5	-20.9

[a]Distances are in Å, angles in degrees, and energies in kJ/mol; the labeling of the atoms corresponds to Fig. 2.
[b]Optimized with a very large UCV basis set (1046 function).
[c]Reference 8.
[d]Recommended value from Ref. 22.

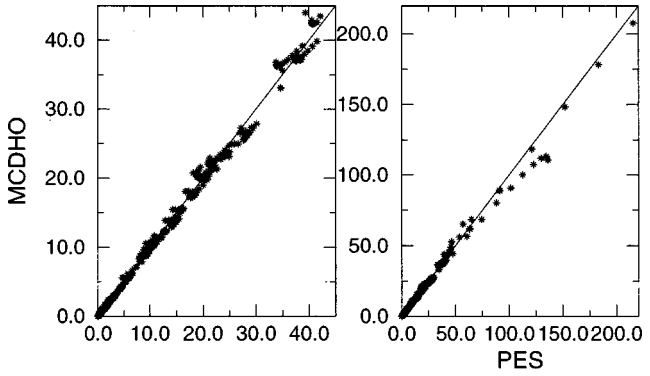

FIG. 3. Comparison of the MCDHO model to the analytical potential energy surface (PES) of Ref. 63. Left: reproduction of the sample that was fitted. Right: extrapolation of the model to higher deformation energies. Values in kJ/mol.

III. RESULTS

In this section we discuss the ability of the MCDHO model to reproduce the water–water interactions, by studying *ab initio* surfaces of the intermolecular interactions, the structures, energies and dipoles of clusters, the second virial coefficient, and a numerical simulation of the liquid under ambient conditions.

A. Monomer deformation energies and dipoles

As a first test, we extended the sampling of the monomer deformation energy surface to larger values, up to 200 kJ/mol, for a total of 536 points. The comparison to the model's predictions is shown in Fig. 3. The root-mean-square error is $e_{\mathrm{rms}}=2.5$ kJ/mol, so even the extrapolation of the model reproduces well the deformation energies.

The dipoles corresponding to the 536 monomers were obtained from an analytical dipole moment surface (DMS),[63] and the comparison to the model's predictions is shown in Fig. 4. Three regions can be distinguished: a first one with values lower than the dipole in the equilibrium geometry, where the model's predictions lie slightly below the DMS, a second region around 2.0 D, where the model's values follow a pattern that agglomerates above the DMS, and a third region above 2.0 D, where the model's values are somewhat higher than the DMS. The analysis of the pattern around 2.0 D showed that these dipoles correspond to geometries with O–H bonds elongated more than 0.15 Å with respect to the equilibrium monomer; for these geometries the dipole moment actually decreases because there is less charge transfer from the hydrogens; the asymptotic limit of this process leads to three electrically neutral atoms, thus a null total dipole moment. The failure of the MCDHO model to reproduce this dwindling is due to the fact that the true electron density of water is not spherical[60,68,69] and that the mobile charge of the model cannot be split between the oxygen and the hydrogen nuclei, therefore not reproducing the charge transfer. On the other hand, the model can reproduce better the effect of contraction of the O–H bonds because then the equilibrium position of the mobile charge is closer to the oxygen atom, and this mimics the enhanced charge transfer from the hydrogens. Therefore, the model is still useful for a wide range of monomer geometries that can be expected in the gas, liquid, and solid phases under various thermodynamical conditions, as will be shown later.

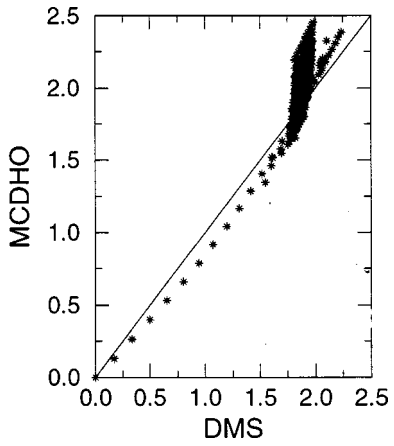

FIG. 4. Comparison of the MCDHO model to the dipole moment surface (DMS) of Ref. 63. Values in Debye.

B. Pair energies

A second test of the model is the comparison to an *ab initio* surface of the pair interaction energies. We used an aug-cc-pVQZ′ basis[70] with a total of 312 functions for two water molecules (the prime denotes that the exponents and coefficients of the *G* functions on oxygen, corresponding to the full aug-cc-pVQZ basis, were used as additional *S* functions).[25,28,70] Including the correlation energy up to the second order of the many-body perturbation theory (MP2), and the CP correction, we found a dimerization energy of −19.7 kJ/mol. Hence, our *ab initio* calculation is close to the theoretical limit of the dimerization energy, −20.8 kJ/mol. However, for an O–O separation of 2.38 Å along the hydrogen bond (HB) line our calculation of the interaction energy between rigid molecules is 15.1 kJ/mol, only 64% of the value reported by Mas and Szalewicz,[27] 23.6 kJ/mol. Such a large discrepancy is most likely due to the known difficulty to reproduce close encounters between molecules. Thus, the short-range energies both at the *ab initio* level and with the MCDHO model are subject to some uncertainty. The effect that would be expected from an underestimation of the short-range repulsion is a low pressure in the simulation of the liquid. In fact, the empirical models that are fitted to reproduce the pressure with 12–6–1 analytical formulas, usually yield a deep minimum that allows for low energies at separations shorter than the minimum. On the other hand, some *ab initio* models use exponential terms for the short range repulsion. These terms approach finite values as the distance shortens, whereas the Coulombic interactions approach a singularity, thus conducing to a collapse of oppositely charged sites.[45,47,57]

With the above remarks in mind, we decided to compare the model against a sample of 736 points in the pair interaction energy surface, that were computed with the previously described *ab initio* protocol. The intermolecular separations in the sample ranged from 2.54 Å, where the interaction energy along the HB line is lower than 10 kJ/mol, to 10.0 Å. This sample included the HB line, the geometries in the

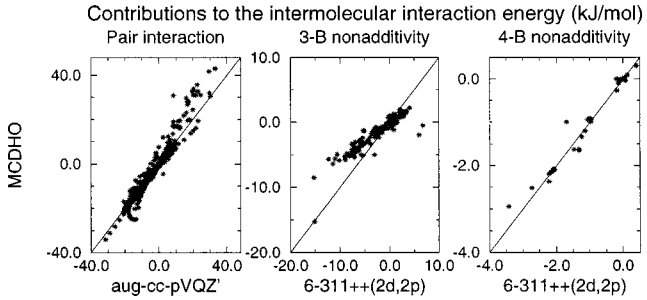

FIG. 5. Comparison of the MCDHO model to samples in the *ab initio* surfaces of pair interactions (left), and the three-body (center) and four-body (right) nonadditive contributions to the interaction energy.

MCY surface, various different pairs of rigid and deformed molecules that appear in equilibrium clusters from trimers to hexamers, and pairs that were taken from simulations of liquid water with the MCHO model.[47] The interaction energy was computed with a many-body expansion that accounts for deformed molecules:[71]

$$\Delta U_n = U_n - \sum_{i=1}^{n} U_i$$

$$= \sum_{i=1}^{n} \delta_i + \sum_{i=1}^{n} \sum_{j>i} V'_{i,j} + \sum_{i=1}^{n} \sum_{j>i} \sum_{k>j} \epsilon'_{i,j,k} + \cdots, \quad (7)$$

where δ_i is the deformation energy of a monomer, and the primes on the subsequent terms denote that the reference single-molecule energies are those of the deformed monomers. With this expansion the energies of the sample range from -33 to 33 kJ/mol, and these extreme values correspond to pairs of quite deformed molecules, with deformation energies up to 40 kJ/mol.

The comparison of the model to the *ab initio* surface is shown in Fig. 5. The points lie on a straight line of slope $m=1.08$, and the standard error is small, $e_{\mathrm{rms}}=2.6$ kJ/mol. At shorter distances, the MCDHO model produces more repulsive values for the energy. For instance, at an O–O separation of 2.38 Å along the hydrogen-bond line, our *ab initio* result is of 15.1 kJ/mol, whereas the MCDHO energy is 45.9 kJ/mol.

C. Many-body nonadditive effects

Instead of adding specific functional forms for the nonadditive effects, the model has built-in polarizability, and its predictions can be compared to *ab initio* results. We generated samples of 174 trimers and 34 tetramers, that result from equilibrium clusters up to hexamers. The nonadditive contribution to the interaction energy was computed from the many-body expansion in Eq. (7).

Because of the large computational cost of the aug-cc-pVQZ' basis, and because the nonadditive effects are less dependent on the size of the basis set,[71] we used a smaller 6-311++G(2*d*,2*p*) basis,[72] including correlation at the MP2 level and the CP correction. The comparison of the model to the *ab initio* surfaces is presented in Fig. 5. In the case of the three-body surface, the standard error is somewhat large, $e_{\mathrm{rms}}=2.4$ kJ/mol, and the points lie along a line with slope $m=0.6$; i.e., the model accounts for only 60% of the three-body nonadditive contribution to the interaction energy, but reproduces the trends well. This modest agreement is imputable again to the sphericity of the mobile charge density of the model, that cannot reproduce the deformations of the electron cloud to be expected in the polarization of flexible molecules. However, the model is still satisfactory in three respects: it accounts for a large part of the three-body nonadditivity, it reproduces the trend from negative to positive values, and it does not exaggerate these values, a risk always present with a built-in polarizability.

In the case of the four-body surface (Fig. 5), the model performs much better: the standard deviation is of only $e_{\mathrm{rms}}=0.2$ kJ/mol and the points lie along a line with slope $m=0.96$.

TABLE V. Reproduction of the water trimer.[a]

	Ref. 29[b]	Ref. 30[c]	Ref. 33[d]	Ref. 31[e]	Expt.[f]	MCDHO
r(O–O)	2.830	2.799		2.782	2.960	2.911
r_{HB}	1.952	1.907		1.896		2.043
$r(\mathrm{O–H})_f$	0.966	0.964		0.958		0.959
$r(\mathrm{O–H})_b$	0.976	0.978		0.972		0.978
θ(H–O–H)	105.3	105.3		105.6		104.1
θ(O–H–O)	148.3	150.3		151.2	152.0	146.9
$\theta(\mathrm{H}_f\mathrm{–O–O–O})$	42.9	56.6		46.4		65.0
$\theta(\mathrm{H}_b\mathrm{–O–O–O})$		6.1		1.9	0.0	1.0
Interaction energy	−61.9	−62.1	−59.6	−66.5		−58.5

[a]Distances are in Å, angles in degrees, and energies in kJ/mol; the values presented are averaged over the three monomers. The subindex *f* refers to the ''free'' hydrogen, whereas *b* stands for the hydrogen engaged in the hydrogen bond.
[b]Computed with a DZP+diff basis set.
[c]Computed with an aug-cc-pVDZ basis.
[d]Computed at the MP2/aug-cc-pVTZ level.
[e]Geometry optimized with an aug-cc-pVQZ basis; the interaction energy was estimated as the limit when increasing the basis set size to ∞.
[f]Reference 11, vibrationally averaged from harmonic frequencies.

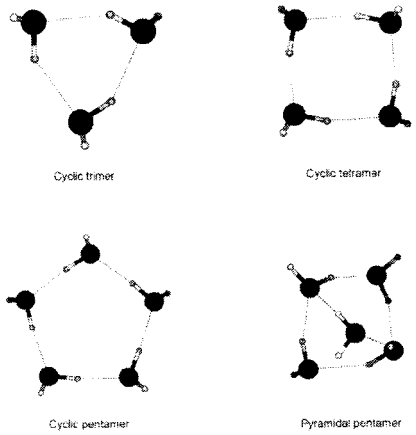

FIG. 6. Optimal water clusters of up to five molecules, found with the MCDHO model. The geometric parameters and energies are shown in Tables V to VII.

D. Water clusters

The optimal structures of water clusters can be predicted by the model, using a Monte Carlo energy minimization, i.e., starting from random geometries at high temperatures ($T=300\,\mathrm{K}$) and gradually lowering the value to $T=0\,\mathrm{K}$.

As we saw, the fitting procedure yields a good reproduction of the monomer (Table II) and an energy difference of only 0.08 kJ/mol with respect to the experimental geometry, so we can confidently keep this latter as the reference in the numerical simulations. The equilibrium dimer, as discussed previously, yielded quite good results. Now we look into larger clusters.

In the following comparisons it is worth noticing that the theoretical O–O distances correspond to well-defined minima, whereas the experimental values include vibrational averaging in an asymmetric potential well, a fact that makes them longer than the theoretical values.

In Table V we compare the model's predictions to the *ab initio* and the experimental trimers. The trimer obtained with the largest basis set is a rather compact structure. The MCDHO model correctly reproduces the cyclic trimer as the minimum (Fig. 6), with slightly longer O–O distances than their *ab initio* counterpart, $\Delta r=0.081\,\text{Å}$. The interaction energy, −58.5 kJ/mol, falls short of the *ab initio* theoretical limit,[31] −66.5 kJ/mol, and the ASP-W2 model,[33] −66.4 kJ/mol, by 8 kJ/mol, but it is quite similar to the value obtained at the MP2/aug-cc-pVTZ level by Hodges *et al.*[33] and to the value produced by their ASP-W4 model (−61.7 kJ/mol). The lack of full agreement can be attributed to the steepness of the short-range repulsion term of the model, that impedes the close approximation of the molecules. However, the total dipole of the trimer is predicted by the model as $\mu=1.144\,\mathrm{D}$, with an average per-molecule $\langle\mu\rangle=2.270\,\mathrm{D}$, very similar to the *ab initio* values,[67] $\mu=1.071\,\mathrm{D}$ and $\langle\mu\rangle=2.3\,\mathrm{D}$.

The model also yields a cyclic water tetramer (Fig. 6), in agreement with both experiment[12] and *ab initio* calculations[30] (Table VI), with slightly longer intermolecular separations ($\Delta r=0.017\,\text{Å}$). Once again, the MCDHO energy, −108.2 kJ/mol, falls short of the ASP-W2 model[33] (−115.4 kJ/mol), but is in better agreement with the ASP-W4 model[33] (−106.7 kJ/mol), and a quantum calculation at the MP2/aug-cc-pVTZ level[33] (−106.0 kJ/mol). Again, the predictions of total dipole, $\mu=0.024\,\mathrm{D}$, and per-molecule, $\langle\mu\rangle=2.528\,\mathrm{D}$, compare well to the *ab initio* values,[67] $\mu=0\,\mathrm{D}$ and $\langle\mu\rangle=2.5\,\mathrm{D}$.

The water pentamer presents two equilibrium geometries, the cyclic and the pyramidal, that are reproduced by the MCDHO model (Fig. 6). It also reproduces the shortening of the O–O distances observed experimentally.[10] This time, it can be seen in Table VII that the MCDHO interaction energy for the cyclic configuration, −147.7 kJ/mol, is larger than the MP2/aug-cc-pVDZ calculation,[33] −139.5 kJ/mol, and the ASP-W4 model, −136.9 kJ/mol, and closer to the ASP-W2 (−146.8 kJ/mol). This also happens for the pyramidal configuration: −139.4 kJ/mol vs. −132.1 kJ/mol (*ab initio*), −146.9 kJ/mol (ASP-W2), and −137.2 kJ/mol (ASP-W4). It is to be noted that the model favors the cyclic pentamer as the global minimum, whereas ASP-W2 and ASP-W4 favor the pyramidal pentamer. We should mention that the experimentally determined global minimum is the cyclic pentamer.[13] For this latter, the *ab initio* values[67] of the total and per-molecule dipoles are $\mu=0.927\,\mathrm{D}$ and $\langle\mu\rangle$

TABLE VI. Reproduction of the water tetramer.[a]

	Ref. 30[b]	Ref. 33[c]	Expt.[d]	MCDHO	ASP-W2	ASP-W4
r(O–O)	2.743		2.790	2.806		
r_{HB}	1.758			1.842		
$r(\mathrm{O-H})_f$	0.965			0.960		
$r(\mathrm{O-H})_b$	0.985			0.986		
θ(H–O–H)	105.0			103.8		
θ(O–H–O)	167.7			164.7		
$\theta(\mathrm{H}_b\mathrm{-O-O-O})$	0.4			0.1		
$\theta(\mathrm{H}_f\mathrm{-O-O-O})$	112.4			112.9		
Interaction energy	−99.6	−106.0		−108.2	−115.4	−106.7

[a]Distances in Å, angles in degrees and energies in kJ/mol; the values presented are averaged over the four monomers. The subindexes *f* and *b* have the same meaning as for the trimer.
[b]Computed at the MP2/aug-cc-pVDZ level. The values of ASP-W2 and ASP-W4 were taken from the same reference.
[c]Computed at the MP2/aug-cc-pVTZ level.
[d]Reference 12, vibrationally averaged structure.

TABLE VII. Reproduction of the water pentamer.[a]

	Geometry		
	Cyclic		Pyramidal
	Ref. 30[b]	MCDHO	MCDHO
r(O–O)[c]	2.867	2.753	2.869
r_{HB}	1.913	1.766	1.947
$r(O–H)_f$	0.943	0.961	0.961
$r(O–H)_b$	0.954	0.991	0.981
θ(H–O–H)	106.2	103.7	103.7

	Interaction energy			
	Ref. 33[d]	ASP-W2	ASP-W4	MCDHO
Cyclic	−139.5	−146.8	−136.9	−147.7
Pyramidal	−132.1	−146.9	−137.2	−139.4

[a]Distances in Å, angles in degrees, and energies in kJ/mol; the values are averaged over the five monomers. The subindexes *f* and *b* have the same meaning as for the trimer.
[b]Geometry optimized at the HF/aug-cc-pVDZ level.
[c]The experimental (Ref. 13) vibrationally averaged result is 2.760 Å.
[d]Computed at the MP2/aug-cc-pVDZ level. The values of ASP-W2 and ASP-W4 were taken from the same reference.

$=2.63$ D, whereas the model predicts $\mu=0.922$ D and $\langle\mu\rangle=2.689$ D.

The hexamer presents a wider variety of configurations, whose *ab initio* energies are in the interval -186.5 ± 2.1 kJ/mol. The structures found with the model are the ring, book, bag, cage, and prism that have been reported[32] (Fig. 7). The geometric parameters and interaction energies are shown in Table VIII. The agreement of MCDHO with both *ab initio* calculations[32] and experimental[14] data is quite good, with a standard error of $e_{rms}=3.5$ kJ/mol, defined as the difference between the energies predicted by the model and their *ab initio* counterparts, though the model favors the cyclic (ring) configuration, whereas the prism and cage are proposed to be the overall minima.[32] The results found by Dang and Chang[56] with a rigid polarizable model have an even larger deviation from the *ab initio* results, $e_{rms}=18.1$ kJ/mol, but a better agreement in the order of their predicted energies, prism (−171.4 kJ/mol)<cage (−170.5 kJ/mol)<book (−169.0 kJ/mol)<cyclic (−164.6 kJ/mol). However, their model does not produce the bag structure.

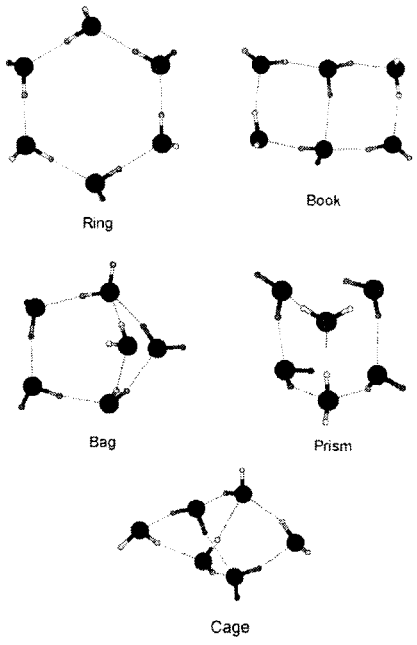

FIG. 7. Stationary water hexamers found with the MCDHO model. The geometric parameters and energies are shown in Table VIII.

TABLE VIII. Reproduction of the water hexamers.[a]

	Ref. 32	MCDHO	Ref. 32	MCDHO
	Ring		Book	
r(O–O)	2.714	2.731	2.766	2.809
r_{HB}	1.734	1.735	1.805	1.849
$r(O–H)_f$	0.958	0.961	0.960	0.960
$r(O–H)_b$	0.980	0.992	0.976	0.985
θ(H–O–H)	105.3	103.5	105.4	102.6
Interaction energy[b]	−183.6	−185.2	−187.2	−184.0
	Bag		Prism	
r(O–O)	2.769	2.812	2.840	2.892
r_{HB}	1.811	1.850	1.956	2.001
$r(O–H)_f$	0.958	0.961	0.958	0.961
$r(O–H)_b$	0.977	0.986	0.972	0.979
θ(H–O–H)	105.2	103.5	104.5	103.2
Interaction energy[b]	−184.5	−183.8	−188.8	−184.9
	Cage			
r(O–O)	2.807	2.888		
r_{HB}	1.876	1.944		
$r(O–H)_f$	0.958	0.961		
$r(O–H)_b$	0.975	0.981		
θ(H–O–H)	105.3	103.7		
Interaction energy[b]	−188.4	−182.8		

[a]Distances are in Å, angles in degrees, and energies in kJ/mol. The numbers presented are averages over the six monomers. The subindexes *f* and *b* have the same meaning as for the trimer.
[b]The *ab initio* structures were optimized at the MP2/TZ2P++ level and the energies obtained from single point calculations at the MP2(FC)/HZ4P(2 *fg*,2*d*)++ level. The experimentally determined (Ref. 14) r(O–O) distance for the cyclic hexamer is 2.756 Å, whereas that of the cage II hexamer is 2.820 Å.

Also, the remarkably good agreement of the MCDHO model predictions of total and per-molecule dipoles with the *ab initio* values[67] is found again for the hexamers. This general good agreement can be appreciated in Table IX, where the model predictions are compared to the available experimental and theoretical values. Thus, the polarizability is adequately taken into account in the model.

E. The second virial coefficient

As mentioned in the introduction, there does not exist in the literature a water model that can reproduce simultaneously the second virial coefficient of steam and the structure and thermodynamic properties of the liquid under ambient conditions.[73] The second virial coefficient quantum corrected to order $\hbar^2$ can be written[73,74] as the sum of a classical contribution and the translational and rotational first quantum corrections,

TABLE IX. Reproduction of the total (μ) and per-molecule ($\langle\mu\rangle$) dipole moments of water clusters.[a]

	μ			$\langle\mu\rangle$		
	Theoret.[b]	Expt.[c]	MCDHO	Theoret.[b]	Expt.[c]	MCDHO
Dimer	2.683	2.643	2.681	2.1		2.086
Trimer	1.071		1.144	2.3		2.270
Tetramer	0		0.024	2.5		2.528
Cyclic pentamer	0.927		0.922	2.6		2.689
Hexamers:						
Ring	0		0.134	2.7		2.791
Cage	2.05	1.904	2.034	2.6		2.553
Prism	2.701		2.627			2.558
Liquid				3.0	2.6	3.01

[a]Values in Debye.
[b]The dipoles for the clusters were computed at the MP2/aug-cc-pVDZ level in Ref. 72; the per-molecule values were taken from Fig. 3 of Ref. 72, whereas the value for the bulk was taken from Ref. 54.
[c]The experimental value for the dimer was taken from Ref. 8 and for the cage hexamer from Ref. 14. The experimental value in liquid water is interpreted from measurements of the dielectric constant (Ref. 54).

$$B_{\rm cl}(T) = -2\pi \int_0^\infty \left\langle \exp\left(\frac{-U_{1,2}}{kT}\right) - 1 \right\rangle_{\omega_1\omega_2} r^2\, dr,$$

$$\Delta B_{\rm tr}(T) = \frac{\hbar^2}{24(kT)^3} \frac{\langle \mathbf{F}^2\rangle_0}{M}, \tag{8}$$

$$\Delta B_{\rm rot}(T) = \frac{\hbar^2}{24(kT)^3} \sum_\alpha \frac{\langle \tau_\alpha^2\rangle_0}{I_{\alpha\alpha}},$$

where $U_{1,2}$ is the pair-interaction energy; $\mathbf{F}$ is the force on one molecule; M the molecular mass; τ_α the component in the molecular inertial axis reference frame of the torque about the α-axis of one molecule for which the moment of inertia is $I_{\alpha\alpha}$; $\hbar$ is Planck's constant, k is Boltzmann's constant, and T the temperature. The brackets $\langle\,\rangle_{\omega_1\omega_2}$ mean the average of the Mayer function over the orientations and geometries ω_1 and ω_2 of the two water molecules at an intermolecular separation r. The brackets $\langle\,\rangle_0$ mean the low density limit.

In this work we used the Monte Carlo numerical integration scheme described by Millot *et al.* in Ref. 73 to obtain the values shown in Tables X, XI, and XII. As an example of the improvement over *ab initio* and empirical models, especially at low temperatures, the MCDHO predictions are compared to the MCHO[47] and SPC/E[43] models in Table X. This improvement should be expected from a better description of the pair-interaction energies, as is the case for the ASP-W2 and ASP-W4 models.[73] The translational and rotational quantum corrections are presented in Table XI, and it can be seen in Table XII that the MCDHO quantum corrected values match quantitatively the experimental data,[75,76] as is also the case for the ASP-W4 model.

Though not a very stringent test at low temperatures, because the slope becomes very steep,[76] the reproduction of the second virial coefficient gives us confidence on the pair interactions predicted by the MCDHO model. In fact, the comparison to the data of Millot *et al.*[73] shows that it performs much better than several empirical and *ab initio* potentials.

F. Liquid water under ambient conditions

As a final and more stringent test, the MCDHO model was used in Monte Carlo simulations of 1000 water molecules in the NVT ensemble, at a temperature of $T = 298.15$ K and the experimental density, $\rho = 0.997$ g/cm^3. Periodic (toroidal) boundary conditions and a spherical cutoff radius of $R_{\rm ct} = 1.085$ nm were used for a cubic box of length $L = 3.106$ nm. The long range Coulombic interaction energies were handled with Ewald sums.[77] The induced polarization requires the zeroing of a force equation for each mobile charge in the simulation cell. In principle, the electrostatic forces should also be handled with Ewald sums, but this would require the time-consuming evaluation of the terms in the reciprocal space every time a charge is displaced, thus making very expensive the self-consistent search for the equilibrium positions. In this work we computed the induced dipole moment of a molecule in the simulation cell, considering the electrostatic contribution due only to the neighboring molecules within a sphere of radius $R_{\rm ct}$; we then increased the value of $R_{\rm ct}$ until the induced dipole did not vary in more than 1%, and arrived at $R_{\rm ct} = 1.085$ nm. This result shows that most of the induced polarization is due to local effects, reflecting the homogeneity and the isotropy of liquid water: after some distance from a molecule, the other water molecules are randomly distributed in concentric spherical shells, so their contribution to the force acting on the mobile charge adds up to zero. Thus, in the numerical simulations we solved for the force whose electrostatic contribution is due only to the neighboring molecules within the cutoff sphere. Of course, this approximation should be the subject of further study. Furthermore, because the induced polarization was computed only for the trial molecule in the Monte Carlo simulation, large equilibration runs (10^8 configurations) were needed. Each million configurations required two hours of CPU RISC 10000, that is four times as much as the SPC/E model, but only one fourth of the MCHO model.

The results of the simulations under the conditions described above were taken from a large statistical sample of 2.5×10^8 configurations. The standard error was computed from a partition of the sample into five blocks of 5×10^7 configurations each. The predicted per-molecule energy without quantum corrections is -43.5 ± 0.06 kJ/mol, that compares rather well to the value of -41.4 kJ/mol, determined from the experimental vaporization enthalpy.[78] It is worth mentioning that there has been some discussion on the size of the quantum corrections,[38,35,79] that lead to conclude that the energy of a classical simulations should be ~ -44.0 kJ/mol. Because the MCDHO model includes intramolecular flexibility, a further study of the change in rotational and vibrational frequencies upon evaporation is needed to settle this matter, but this goes beyond the aim of the present study.

The configurational specific heat predicted by the model is $C_v' = 44.8\pm10.9$ J/mole·K, which is larger than that

TABLE X. Classical second virial coefficient $B_{cl}(T)$ of water[a] for the potentials MCDHO, ASP-W2,[b] ASP-W4,[b] MCHO,[c] and SPC/E.[d]

T/K	MCDHO	ASP-W2	ASP-W4	MCHO	SPC/E
373.15	−580.5	−528.4	−505.0	−1057.8	−1054.7
423.15	−316.3	−331.4	−318.8	−599.9	−600.3
448.15	−254.4	−272.4	−262.7		
473.15	−211.3	−228.1	−220.4	−381.5	−386.9
523.15	−155.2	−166.8	−161.6	−260.7	−269.4
573.15	−116.5	−127.2	−123.4	−186.8	−197.3
673.15	−70.8	−80.1	−77.8	−104.0	−115.9
773.15	−50.8	−53.8	−52.3	−60.5	−72.6
873.15	−40.0	−37.4	−36.2	−34.7	−46.3

[a]Values are in cm^3/mole.
[b]Reference 73.
[c]Reference 47.
[d]Reference 43.

obtained from previous *ab initio* models,[47] $C'_v = 33.9$ J/mole·K, and closer to the experimental value of 74.9 J/mole·K, as should be expected because of the inclusion of more degrees of freedom, thus producing larger fluctuations in energy. However, it should be kept in mind that the Monte Carlo simulations include only the variations of potential energy. A further study of rotations and vibrations will be done by means of molecular dynamics.[80]

With respect to the structure of the liquid, the radial distribution functions (rdf's) $g_{OO}(r)$, $g_{OH}(r)$, and $g_{HH}(r)$ produced by the MCDHO model are compared to the results obtained from neutron diffraction data,[19] in Fig. 8:

(1) It can be seen that the agreement with the experimental $g_{OO}(r)$ is very good, not only in the locations, but in the heights of the maxima;
(2) The locations of the maxima of $g_{OH}(r)$ coincide with the experimental ones, but the peaks are slightly higher, which seems to be a general feature of various models;[34]
(3) In the case of $g_{HH}(r)$, there is a general agreement of the same quality as other *ab initio* potentials,[46–48] but still with a third small peak, that does not match the experimental curve, and is also present in the MCHO model.[47]

TABLE XI. Quantum corrections for the second virial coefficient $B(T)$ of water[a] for the MCDHO model compared to the ASP-W2 and ASP-W4 values.[b]

	$\Delta B_{tr}(T)$[c]			$\Delta B_{rot}(T)$[d]		
T/K	MCDHO	ASP-W2	ASP-W4	MCDHO	ASP-W2	ASP-W4
373.15	9.2	6.3	5.9	89.8	77.7	84.1
423.15	3.6	3.0	2.8	32.3	36.9	40.3
448.15	2.5	2.2	2.1	20.4	27.0	29.5
473.15	1.8	1.6	1.6	12.0	20.4	22.3
523.15	0.9	1.0	1.0	6.4	12.4	13.7
573.15	0.5	0.7	0.7	4.2	8.2	9.0
673.15	0.2	0.4	0.3	1.4	4.1	4.6
773.15	0.1	0.2	0.2	0.7	2.4	2.7
873.15	0.1	0.1	0.1	0.4	1.6	1.8

[a]Values are in cm^3/mole.
[b]Reference 73.
[c]Correction from the translational molecular degrees of freedom.
[d]Correction from the rotational molecular degrees of freedom.

TABLE XII. Comparison of the quantum corrected second virial coefficient[a] $B(T)$ of the MCDHO model to the ASP-W2 and ASP-W4 models,[b] and to experimental data.

T/K	MCDHO	ASP-W2	ASP-W4	Expt.[c]	Expt.[d]
373.15	−481.5	−444.3	−415.0		−440.7
423.15	−280.4	−291.4	−275.7	−275.0	−283.6
448.15	−231.5	−243.2	−231.1	−239.5	−235.9
473.15	−197.5	−206.1	−196.5	−200.8	−199.8
523.15	−147.9	−153.4	−147.0	−149.8	−149.3
573.15	−111.8	−118.3	−113.7	−115.8	−116.2
673.15	−69.2	−75.6	−72.9	−73.5	−76.0
773.15	−50.0	−51.2	−49.3	−49.9	−52.8
873.15	−39.5	−35.7	−34.3		−37.7

[a]Values are in cm^3/mole.
[b]Reference 73.
[c]Reference 75.
[d]Reference 76.

A more stringent test of the predictions on structure is the comparison to the directly measured x-ray and neutron diffraction structure functions, that can be obtained from the partial structure factors $H_{\alpha,\beta}(Q)$, which are the Fourier transforms of the corresponding rdf's:[19]

$$H_{\alpha,\beta}(Q) = 4\pi\mathcal{N}\int_0^\infty r^2(g_{\alpha,\beta}(r)-1)\frac{\sin(Qr)}{Qr}dr, \tag{9}$$

where Q is the wave-vector change in the diffraction experiment, and $\mathcal{N}$ is the number density ($\mathcal{N}=0.0334$ molecules/Å^3). The structure function is computed as

$$H_{H_2O}(Q) = \frac{\Sigma_\alpha\Sigma_\beta c_\alpha c_\beta f_\alpha(Q) f_\beta(Q) H_{\alpha,\beta}(Q)}{\langle F^2(Q)\rangle}, \tag{10}$$

where c_α and $f_\alpha(Q)$ are the atomic fraction and scattering length of atomic species α, respectively, and $\langle F^2(Q)\rangle$ is the mean-square scattering length of one water molecule:

$$\langle F^2(Q)\rangle = \sum_{\alpha=1}^{3}\sum_{\beta=1}^{3} f_\alpha(Q) f_\beta(Q) \times \exp(-b_{\alpha,\beta}Q^2)\frac{\sin(Qr_{\alpha,\beta})}{Qr_{\alpha,\beta}}, \tag{11}$$

that depends only on the intermolecular distribution of scattering density, described by the average interatomic distances $r_{\alpha,\beta}$ and their mean-square variations $2b_{\alpha,\beta}$.

We used the radial distribution functions from the neutron diffraction experiment of Soper *et al.*,[19] and those from the MCDHO model to compute the structure functions. The x-ray atomic scattering lengths depend on the wave-vector change Q, so we employed the experimental data of Narten and Levy.[81] The data for the neutron scattering lengths for oxygen, hydrogen, and deuterium are[81,82] $f_O = 0.577 \times 10^{-14}$ m, $f_H = -0.374 \times 10^{-15}$ m, and $f_D = 0.667 \times 10^{-14}$ m, respectively. We employed the intermolecular distances of the isolated water molecule, $r_{OH} = 0.9572$ Å and $r_{HH} = 1.5139$ Å, with the mean-square deviations $b_{OH} = 0.0011$ Å and $b_{HH} = 0.0033$ Å. The comparison of the various structure functions is presented in Fig. 8.

The experimental x-ray structure function[81] is well-reproduced by the Soper's functions, to the point that it can-

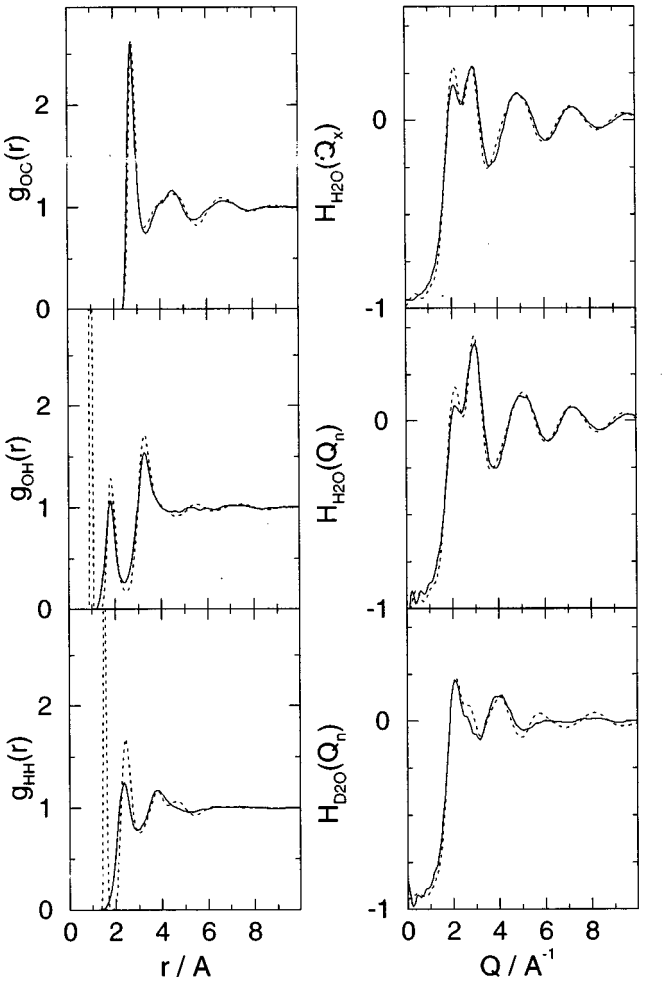

FIG. 8. Comparison of the radial distribution functions (left) and the structure functions (right) obtained with the MCDHO model (dotted line) to the experimental results of Soper *et al.* (Ref. 19) (continuous line), for liquid water at $T=298.15$ K and $\rho=0.997$ g/cm^3. On the right, from top to bottom, x-ray structure function, neutron scattering structure function for light water, and neutron scattering structure function for heavy water. The x-ray experimental data of Narten and Levy (Ref. 81) overlap Soper's functions.

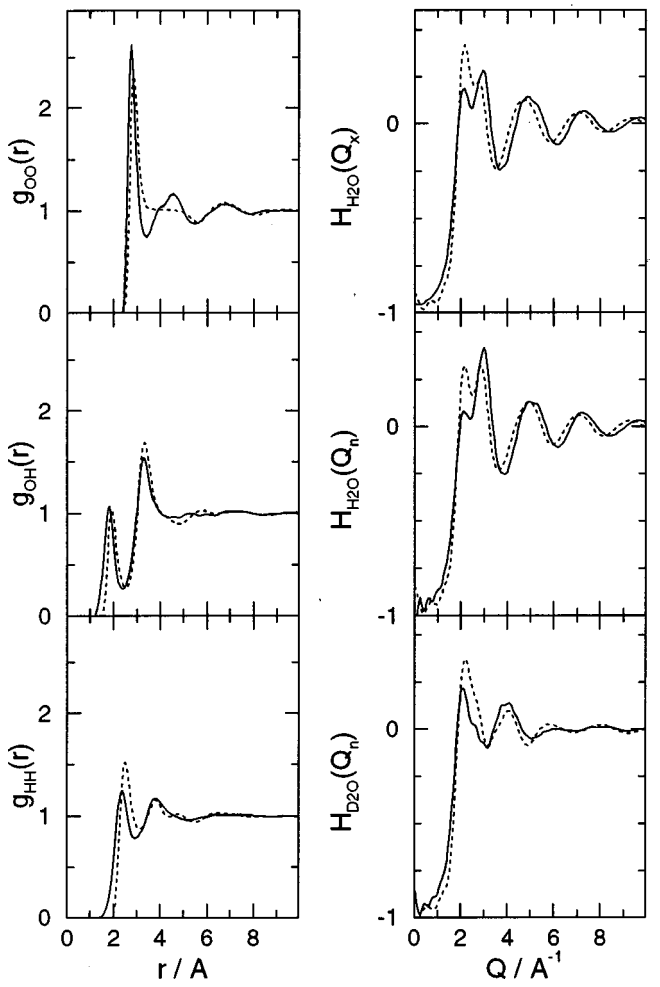

FIG. 9. Same as in Fig. 8, for the predictions of the rigid version of the MCDHO model (dotted line).

not be distinguished in Fig. 9. The MCDHO model performs almost equally well, except for a more pronounced first peak; however, it corrects the depth of the first minimum of the MCHO model.[47] With respect to the neutron diffraction structure function for light water, MCDHO slightly exaggerates the first two maxima and the minimum between them.

Finally, the neutron diffraction structure function for heavy water, D_2O, was computed under the assumption that both the molecular geometry and the intermolecular and intramolecular interactions are the same as those of light water. The MCDHO prediction matches the first two maxima and the minimum in between, and corrects an intermediate maximum produced by MCHO. However, it produces further maxima where Soper's functions seem rather flat. A closer look shows that the Soper's functions also produce those maxima, but with lower values.

To obtain the density predicted by the model, additional Monte Carlo simulations were made with 512 molecules in the NPT ensemble, at $T=298.15$ K and $P=1$ atm (101.325 kPa). The MCDHO value for the predicted density, $\rho=1.02\pm0.01$ g/cm^3, is in good agreement with experiment, and certainly an improvement over most previous *ab initio* based models: for comparison, the same simulation was done with the MCHO model and a lower density, $\rho=0.89$ g/cm^3, was obtained.

The per-molecule dipole moment of the model is somewhat high, $\mu=3.01\pm0.01$ D, but this is in agreement with a recent simulation with a DFT force field.[54] This latter simulation, and the excellent agreement of the MCDHO predictions with the dipoles of water clusters presented in Table X, support the conclusion that the *ab initio* prediction for the dipole moment of water molecules in the liquid might be this high. However, it could also be due to the handling of long-range forces,[83] and should be the subject of further studies.

To check for the effects of flexibility, we restrained the intramolecular motions and performed Monte Carlo simulations of 512 rigid water molecules in the NVT ensemble, at $T=298.15$ K and $\rho=0.997$ g/cm^3. The energy produced by the rigid versions of the model was -42.2 ± 0.3 kJ/mol, still close to the ''experimental'' value, -41.4 kJ/mol.

With regard to the rdf's, the rigid version produces a less structured liquid (Fig. 9): a flat $g_{OO}(r)$ with a first peak shifted to the right. However, the rigid model seems to give

a better agreement with Soper's $g_{OH}(r)$. The behavior of the $g_{HH}(r)$ produced by the rigid model is very similar to its flexible counterpart. The analysis of the structure functions reveals that the seemingly good reproduction of $g_{OH}(r)$ is deceiving: the rigid version of the model inverts the heights of the two first maxima in the x-ray function and also worsens the neutron structure functions for light and heavy water.

The obvious deficiency of the rigid MCDHO contrasts the good performance of previous rigid models. In the case of empirical potentials, the explanation is that the rdf's were used in the adjustment of their parameters. In the case of the *ab initio* potentials, they were fitted to pair interaction surfaces with an exaggerated dimerization energy, ~ -22.6 kJ/mol or even lower, that compensates the lack of molecular relaxation. It is now clear that the proper reproduction of the intermolecular interaction implies the necessity of intramolecular relaxation.

IV. DISCUSSION AND CONCLUDING REMARKS

In this work we propose a new model based on the reproduction of the single molecule properties, *ab initio* calculations of single molecule deformation energies, and the optimal water dimer. We found that though the pair interactions and the four-body nonadditive contributions to the energy are well-reproduced with the assumption of a spherically symmetric electron density, this assumption does not allow for the full reproduction of the three-body nonadditive contributions. The use of a nonspherical charge density might be necessary to overcome this difficulty.

Although Monte Carlo simulations with this model are four times slower than with standard empirical potentials, they can be used for a more refined description of some phenomena, for instance the solvation of monoatomic ions, or the behavior of water under narrow confinement, where both polarizability and intramolecular flexibility are likely to be relevant. In fact, when deformation was not allowed in the numerical simulations, the same model produced less satisfactory results. This is opposite to what has been reported for empirical simple models,[84] in which the effects of both polarizability and flexibility can be included in the parameters, in an averaged manner. However, the models fitted to the liquid in this way cannot be used confidently for the description of other phases. It is worth mentioning that the computational cost of flexibility is negligible, the most expensive part being the calculation of the equilibrium positions of the mobile charges. Alternative methods to predict these positions should be searched.

From the comparison of the MCDHO predictions of water clusters against the most recent experimental and theoretical results, we can conclude that the model has a quality similar to MP2/aug-cc-pVTZ calculations. The second virial coefficient obtained from the MCDHO model shows a clear improvement over previous polarizable, *ab initio* based models. There is also an improvement in the prediction of the density, whereas the quality in reproducing the energy and the structure of the liquid remains basically the same.

It is worth mentioning that to test the model we compared its predictions to samples of *ab initio* potential energy surfaces (PES); an obvious refinement of the model would be to readjust the parameters to reproduce those samples and all the properties already used. We did this and achieved a good reproduction of the samples, and even an improvement in the reproduction of the previously fitted properties, e.g., the polarizability and the intramolecular PES. Interesting enough is the fact that increasing the data in the learning set led to this improvement, instead of the usual worsening that happens when fitting an extended set of data. Nevertheless, this readjustment of the parameters produced a slight worsening in the predictions of the properties of the water clusters, as compared to the ''best'' theoretical and experimental data, the second virial coefficient, and the properties of the liquid. Though the predictions of the model with these parameters were poorer, they were still reasonable. Therefore, we obtained samples of *ab initio* PES's whose fitting leads to a proper reproduction of liquid water; but it is also clear that an improved PES is needed so its sole reproduction would assure an adequate potential.

With respect to the MCDHO predictions of structure, especially the high peaks in the $g_{OH}(r)$ and $g_{HH}(r)$, it should be mentioned that the radial distribution functions are not directly measured, but inferred from the structure functions by means of inverse Monte Carlo fittings,[19] and thus the experimental heights of the maxima are not as reliable as their locations. However, the MCDHO overestimations can also be appreciated in the structure functions, and thus have to be taken as limitations of the model. Nevertheless, it should also be mentioned that here we have presented a reproduction of the experimental $g_{OO}(r)$ and x-ray $H_{H_2O}(Q)$ with the same quality as the best previously reported.

Therefore, we have produced a model, MCDHO, that includes all the molecular degrees of freedom, except an explicit charge transfer, and brings the highest *ab initio* quality thus far obtained to the numerical simulations of the liquid. We showed that this procedure is able to correctly predict several properties of water under various conditions, from water clusters to condensed phases, with increasing accuracy, as the model is refined. Not only this refinement was attained, but also a four-fold lowering in the computational cost with respect to the MCHO model.

ACKNOWLEDGMENTS

This work was supported by the Science Commission of the European Community, under Grant No. CI1*-CT94-0124, by CONACyT, México, under Grant L004-E, and by DGAPA-UNAM, under Grant ES112896. One of us, H.S.-M. thanks the European Community for a bursary for a one-year stay at Rijksuniversiteit Groningen in 1993.

[1] F. Franks, *Water, the Unique Chemical, in Water: A Comprehensive Treatise*, edited by F. Franks (Plenum, New York, 1972), Vol. 1, pp. 1–20.
[2] For instance, the series of books, *Water: A Comprehensive Treatise*, started by F. Franks in 1972.
[3] W. S. Benedict, N. Gailar, and E. Plyler, J. Chem. Phys. **24**, 1139 (1956).
[4] J. Verhoeven and A. Dymanus, J. Chem. Phys. **52**, 3222 (1970).
[5] S. A. Clough, Y. Beers, G. P. Klein, and L. S. Rothman, J. Chem. Phys. **59**, 2254 (1973).
[6] W. F. Murphy, J. Chem. Phys. **67**, 5877 (1977).

[7] I. G. John, G. B. Backsay, and N. S. Hush, Chem. Phys. **51**, 49 (1980).
[8] T. R. Dyke, K. M. Mack, and J. S. Muenter, J. Chem. Phys. **66**, 498 (1977); A. Odutola and T. R. Dyke, *ibid.* **72**, 5062 (1980); J. A. Odutola, T. A. Hu, D. Prinslow, S. E. O'dell, and T. R. Dyke, *ibid.* **88**, 5352 (1988).
[9] L. A. Curtiss, D. J. Frurip, and M. Blander, J. Chem. Phys. **71**, 2703 (1979).
[10] K. Liu, J. D. Cruzan, and R. J. Saykally, Science **271**, 929 (1996).
[11] N. Pugliano and R. J. Saykally, Science **257**, 1937 (1992); M. R. Viant, J. D. Cruzan, D. D. Lucas, M. G. Brown, K. Liu, and R. J. Saykally, J. Phys. Chem. A **101**, 9032 (1997).
[12] J. D. Cruzan, L. B. Braly, K. Liu, M. G. Brown, J. G. Loeser, and R. J. Saykally, Science **271**, 59 (1996); J. D. Cruzan, M. R. Viant, M. G. Brown, and R. J. Saykally, J. Phys. Chem. A **101**, 9022 (1997).
[13] K. Liu, M. G. Brown, J. D. Cruzan, and R. J. Saykally, Science **271**, 62 (1996); J. Phys. Chem. A **101**, 9011 (1997).
[14] K. Liu, M. G. Brown, C. Carter, R. J. Saykally, J. K. Gregory, and D. C. Clary, Nature (London) **381**, 501 (1996); K. Liu, M. G. Brown, and R. J. Saykally, J. Phys. Chem. A **101**, 8995 (1997).
[15] R. N. Pribble and T. S. Zwier, Science **265**, 75 (1994).
[16] F. Huisken, M. Kaloudis, and A. Kulcke, J. Chem. Phys. **104**, 17 (1996).
[17] C. J. Gruenloh, J. R. Carney, C. A. Arrington, T. S. Zwier, S. Y. Fredericks, and K. D. Jordan, Science **276**, 1678 (1997).
[18] U. Buck, I. Ettischer, M. Melzer, V. Buch, and J. Sadlej, Phys. Rev. Lett. **80**, 2578 (1998).
[19] A. K. Soper, F. Bruni, and M. A. Ricci, J. Chem. Phys. **106**, 247 (1997); P. Jedlovszky, J. P. Brodholt, F. Bruni, M. A. Ricci, A. K. Soper, and R. Vallauri, *ibid.* **108**, 8528 (1998); files with the experimental radial distribution functions were kindly provided by F. Bruni, M. A. Ricci, and A. K. Soper.
[20] M. J. Frisch, J. E. del Bene, J. S. Binkley, and H. F. Schaefer III, J. Chem. Phys. **84**, 2279 (1986).
[21] D. Feller, J. Chem. Phys. **96**, 6104 (1992).
[22] J. G. C. M. van Duijneveldt-van de Rijdt and F. B. van Duijneveldt, J. Chem. Phys. **97**, 5019 (1992).
[23] C. Millot and A. J. Stone, Mol. Phys. **77**, 439 (1992).
[24] S. S. Xantheas and T. H. Dunning, Jr., J. Chem. Phys. **99**, 8774 (1993); S. S. Xantheas, *ibid.* **100**, 7523 (1994).
[25] J. E. del Bene and I. Shavitt, in *Molecular Interactions: From van der Waals to Strongly Bound Complexes*, edited by S. Scheiner (Wiley, Sussex, 1997), pp. 157–179.
[26] M. Schütz, S. Brdarski, P. O. Widmark, R. Lindh, and G. Karlström, J. Chem. Phys. **107**, 4597 (1997).
[27] E. M. Mas and K. Szalewicz, J. Chem. Phys. **104**, 7606 (1996).
[28] F. B. van Duijneveldt, in *Molecular Interactions: From van der Waals to Strongly Bound Complexes*, edited by S. Scheiner (Wiley, Sussex, 1997), pp. 81–104.
[29] J. E. Fowler and H. F. Schaefer III, J. Am. Chem. Soc. **117**, 446 (1995).
[30] S. S. Xantheas and T. H. Dunning, Jr., J. Chem. Phys. **98**, 8037 (1993).
[31] I. M. B. Nielsen, E. T. Seidl, and C. L. Janssen, J. Chem. Phys. **110**, 9435 (1999).
[32] J. Kim and K. S. Kim, J. Chem. Phys. **109**, 5886 (1999).
[33] M. P. Hodges, A. J. Stone, and S. Xantheas, J. Phys. Chem. **101**, 9163 (1997).
[34] P. Jedlovszky, J. P. Brodholt, F. Bruni, M. A. Ricci, A. K. Soper, and R. Vallauri, J. Chem. Phys. **108**, 8528 (1998).
[35] V. Buch, P. Sandler, and J. Sadlej, J. Phys. Chem. B **102**, 8641 (1998); J. Sadlej, V. Buch, J. K. Kazimirski, and U. Buck, J. Phys. Chem. A **103**, 4933 (1999).
[36] F. H. Stillinger and A. Rahman, J. Chem. Phys. **60**, 1545 (1974); **68**, 666 (1978).
[37] H. J. C. Berendsen, J. P. M. Postma, W. F. van Gunsteren, and J. Hermans, in *Intermolecular Forces: Proceedings of the Fourteenth Jerusalem Symposium on Quantum Chemistry and Biochemistry*, edited by B. Pullman (Reidel, Dordrecht, 1981), pp. 331–342.
[38] W. L. Jorgensen, J. Chandrasekhar, J. D. Madura, R. W. Impey, and M. L. Klein, J. Chem. Phys. **79**, 926 (1983).
[39] A. Wallqvist and B. J. Berne, J. Phys. Chem. **97**, 13841 (1993).
[40] G. W. Robinson, S.-B. Zhu, and M. W. Evans, *Water in Biology, Chemistry and Physics: Experimental Overviews and Computational Methodologies* (World Scientific, Singapore, 1996).
[41] J. P. M. Postma, Ph. D. thesis, University of Groningen, 1985.
[42] P. Barnes, J. L. Finney, J. D. Nicholas, and J. E. Quinn, Nature (London) **282**, 459 (1979).
[43] H. J. C. Berendsen, J. R. Grigera, and T. P. Straatsma, J. Phys. Chem. **91**, 6269 (1987).
[44] S. W. Rick, S. J. Stuart, and B. J. Berne, J. Chem. Phys. **101**, 6141 (1994).
[45] O. Matsuoka, E. Clementi, and M. Yoshimine, J. Chem. Phys. **64**, 1351 (1976).
[46] U. Niesar, G. Corongiu, E. Clementi, G. R. Kneller, and D. K. Bhattacharya, J. Phys. Chem. **94**, 7949 (1990); G. Corongiu, Int. J. Quantum Chem. **42**, 1209 (1992).
[47] H. Saint-Martin, C. Medina-Llanos, and I. Ortega-Blake, J. Chem. Phys. **93**, 6448 (1990).
[48] A. Wallqvist, Chem. Phys. **148**, 439 (1990); P.-O. Åstrand, A. Wallqvist, and G. Karlström, J. Chem. Phys. **100**, 1262 (1994); P.-O. Åstrand, P. Linse, and G. Karlström, Chem. Phys. **191**, 195 (1995).
[49] A. Famulari, M. Raimondi, M. Sironi, and E. Gianinetti, Chem. Phys. **232**, 275 (1998).
[50] R. Car and M. Parrinello, Phys. Rev. Lett. **55**, 2471 (1985).
[51] P. Hohenberg and W. Kohn, Phys. Rev. **136**, B864 (1964).
[52] K. Laasonen, M. Sprik, M. Parrinello, and R. Car, J. Chem. Phys. **99**, 9080 (1993); M. Sprik, J. Hutter, and M. Parrinello, *ibid.* **105**, 1142 (1996).
[53] G. Lobaugh and G. A. Voth, J. Chem. Phys. **106**, 2400 (1997).
[54] P. L. Silvestrelli and M. Parrinello, J. Chem. Phys. **111**, 3572 (1999).
[55] B. D. Bursulaya and H. J. Kim, J. Chem. Phys. **108**, 3277 (1998); B. D. Bursulaya, J. Jeon, D. A. Zichi, and H. J. Kim, *ibid.* **108**, 3286 (1998).
[56] L. X. Dang and T.-M. Chang, J. Chem. Phys. **106**, 8149 (1997).
[57] E. M. Mas, K. Szalewicz, R. Bukowski, and B. Jeziorski, J. Chem. Phys. **107**, 4207 (1997).
[58] A. Famulari, R. Specchio, M. Sironi, and M. Raimondi, J. Chem. Phys. **108**, 3296 (1998).
[59] Y.-P. Liu, K. Kim, B. J. Berne, R. A. Friesner, and S. W. Rick, J. Chem. Phys. **108**, 4739 (1998).
[60] J. B. Hasted, *Liquid Water: Dielectric Properties, in Water: A Comprehensive Treatise*, edited by F. Franks (Plenum, New York, 1972), Vol. 1, pp. 255–309.
[61] J. Hernández-Cobos, I. Ortega-Blake, M. Bonilla-Marín, and M. Moreno-Bello, J. Chem. Phys. **99**, 9122 (1993); H. Saint-Martin, I. Ortega-Blake, A. Leś, and L. Adamowicz, Biochim. Biophys. Acta **1207**, 12 (1994); M. I. Bernal-Uruchurtu and I. Ortega-Blake, J. Chem. Phys. **103**, 1588 (1995); J. Hernández-Cobos and I. Ortega-Blake, *ibid.* **103**, 9261 (1995); M. L. San-Román and I. Ortega-Blake, *ibid.* **107**, 3253 (1997); M. I. Bernal-Uruchurtu, J. Hernández-Cobos, and I. Ortega-Blake, *ibid.* **108**, 1750 (1998).
[62] D. D. Klug, C. A. Tulk, E. C. Svensson, and C.-K. Loong, Phys. Rev. Lett. **83**, 2584 (1999).
[63] H. Partridge and D. W. Schwenke, J. Chem. Phys. **106**, 4618 (1997).
[64] B. G. Dick, Jr. and A. Overhauser, Phys. Rev. **112**, 90 (1958).
[65] P. C. Jordan, P. J. van Maaren, J. Mavri, D. van der Spoel, and H. J. C. Berendsen, J. Chem. Phys. **103**, 2272 (1995).
[66] R. Fabianski, B. Kuchta, L. Firlej, and R. D. Etters, J. Chem. Phys. **112**, 6745 (2000).
[67] J. K. Gregory and D. C. Clary, Science **275**, 814 (1997).
[68] C. W. Kern and M. Karplus, *The Water Molecule, in Water: A Comprehensive Treatise*, edited by F. Franks (Plenum, New York, 1972), Vol. 1, pp. 21–91.
[69] S. Tanizaki, J. Mavri, H. Partridge, and P. C. Jordan, Chem. Phys. **246**, 37 (1999).
[70] T. H. Dunning, Jr., J. Chem. Phys. **90**, 1007 (1989); R. A. Kendall, T. H. Dunning, Jr., and R. J. Harrison, *ibid.* **96**, 6796 (1992); D. Woon and T. H. Dunning, Jr., *ibid.* **103**, 4572 (1995); Basis sets were obtained from the Extensible Computational Chemistry Environment Basis Set Database, Version 1.0, as developed and distributed by the Molecular Science Computing Facility, Environmental and Molecular Sciences Laboratory which is part of the Pacific Northwest Laboratory, P.O. Box 999, Richland, Washington 99352, and funded by the U.S. Department of Energy. The Pacific Northwest Laboratory is a multiprogram laboratory operated by Battelle Memorial Institute for the U.S. Department of Energy under Contract DE-AC06-76RLO 1830. Contact David Feller or Karen Schuchardt for further information.
[71] N. Pastor-Colón and I. Ortega-Blake, J. Chem. Phys. **99**, 7899 (1993).
[72] R. Krishnan, J. S. Binkley, R. Seeger, and J. A. Pople, J. Chem. Phys. **72**, 650 (1980); T. Clark, J. Chandrasekhar, and P. v. R. Schleyer, J. Comput. Chem. **4**, 294 (1983).

[73] C. Millot, J.-C. Soetens, M. T. C. Martins-Costa, M. P. Hodges, and A. J. Stone, J. Phys. Chem. **102**, 754 (1998).
[74] C. G. Gray and K. E. Gubbins, *Theory of Molecular Fluids Volume I: Fundamentals* (Clarendon, Oxford, 1984), pp. 209–210.
[75] G. S. Kell, G. E. Mc Laurin, and E. J. Whalley, Proc. R. Soc. London, Ser. A **425**, 49 (1989).
[76] A. Ben-Naim, *Statistical Thermodynamics for Chemists and Biochemists* (Plenum, New York, 1992), pp. 472–474.
[77] M. P. Allen and D. J. Tildesley, *Computer Simulations of Liquids* (Oxford Science, London, 1994), pp. 156–162.
[78] D. Eisenberg and W. Kauzmann, *The Structure and Properties of Water* (Oxford University Press, London, 1969).
[79] P. H. Berens, D. H. J. Mackay, G. M. White, and K. R. Wilson, J. Chem. Phys. **79**, 2375 (1983).
[80] Work in progress at our lab.
[81] A. H. Narten and H. A. Levy, J. Chem. Phys. **55**, 2263 (1971).
[82] A. K. Soper, Chem. Phys. **88**, 187 (1984).
[83] P. E. Smith and W. F. van Gunsteren, J. Chem. Phys. **100**, 3169 (1994); P. H. Hünenberger and W. F. van Gunsteren, *ibid.* **108**, 6117 (1998).
[84] I. G. Tironi, R. M. Brunne, and W. F. van Gunsteren, Chem. Phys. Lett. **250**, 19 (1996).